



2011 IEEE Visualization Contest Winner: Visualizing Unsteady Vortical Behavior of a Centrifugal Pump

Mathias Otto¹, Alexander Kuhn¹, Wito Engelke^{1,2}, and Holger Theisel¹

¹University of Magdeburg, ²Kaust

ABSTRACT

This work summarizes our results analyzing a centrifugal pump for the IEEE Visualization Contest 2011. The given data set represents a high resolution simulation of a centrifugal pump operating below optimal speed settings. The goal is to find suitable visualization techniques to identify areas of rotating stall that impede the effectiveness of the pump in practical application. We split our analysis into three parts based on the functional behavior of the pump and applied local and integration based techniques to communicate the unsteady flow behavior in different regions of the data set. Based on this we present a direct comparison of a set of common vortex extractors and more recent approaches and discuss their applicability in this case. Further, we show that integration based methods (namely separation measures, accumulated scalar fields, particle path lines, and advection textures) are well suited to capture the complex time-dependent flow behavior.

1 INTRODUCTION

The given data represents three high resolution simulations using different turbulence models of a centrifugal pump used to transport liquids within pipe systems with a broad range of practical applications. A detailed overview of the simulation settings and physical context is described by Lucius et al. [1]. The main components of this device can be split into an inlet, a moving impeller producing a rotatory motion within the flow, and an area where the accelerated liquid is transported into the outlet region. This functional principal is illustrated in figure 1. Based on this scheme we focus our study on three major aspects of the device: First, we analyzed the behavior of the incoming flow within the inlet area and its transport into the impeller

area in section 2.2. Second, we examine the general flow behavior by means of fluid transport in regions where the liquid is forced into rotating motion by the blade of the impeller (see section 2.3). Finally, we take a general look towards the comparison of the turbulence models for all given simulation models within section 3. We especially focus on the Scale-Adaptive Simulation (SAS) model, as it will be shown to have the most complex turbulence behavior and is assumed to be the model closest to real flow processes [1]. Still, for most of our integration based models we provide a comparative overview of the results. Additionally, we integrated given scalar field values, such as pressure, on path lines to visualize the global flow behavior. In order to answer questions regarding the pump efficiency, we utilized a set of specific visualization methods, tailored towards functional relations between different transport effects. Finally, we conclude with further details about the implemented prototype and visualization tools in section 4.

2 DATA SET ANALYSIS

The given data set is available in Ensign ASCII and Ansys format, including two velocity fields, four common scalar fields and up to three additional method specific fields describing turbulence parameters of the respective simulation models. The fields are stored as a vertex based description on an adaptive hexahedral volume grid containing 6.7 Million nodes and 6.5 Million cells. The data contains one complete circulation of the rotor sampled in 80 time steps taken from a longer simulation run. Note, that due to the strong differences in between the first and last time steps we assume non-periodic flow behavior for the given time interval.

Jan Klein, Fraunhofer MEVIS
Gabriel Zachmann, Clausthal University

The annual IEEE Visualization Contest presents challenging problems to the research community in the hope of obtaining novel solutions. The contest promotes a problem in a different domain each year by providing data and corresponding scientific queries that can be addressed through visualization. Data format documentation and sample reader programs are available for contestants to validate processing and jump-start their work. The contest has become a widely used repository of well-defined scientific problems with open data. Past and upcoming contest data, questions, and submission archives are available at <http://viscontest.sdsc.edu>.

The Contest Problem

The 2011 contest's theme was the stability visualization in the area of centrifugal pumps. The stable operating range of pumps is limited by flow instabilities occurring in deep part load. If the flow rate is reduced the flow onto leading edge is misaligned and stalls at a critical lower limit, similar to the stall of a wing at high angle of attack. Due to interaction of adjacent blade channels the stall rotates at constant rotational speed relative to the blading. The strong fluctuations of fluid flow properties during stall may lead to flow induced vibrations, which need to be avoided. The phenomenon is strongly influenced by turbulence, so turbulence modeling is of vital importance for the simulation of such a flow. The overall goal is to visualize the instability of the flow and help understand the movement and development of rotating stall cells **based on 3 different turbulence models**. The goal is to find a visualization such that researchers can easily gain insights as to **where** these vortices develop, how the stall moves and, possibly, **why** they develop.

2.1 Functional Behavior

According to its practical task the given centrifugal pump can be split into specific regions of different functionality during the running state. The first inlet region guides the flow in a direction orthogonal to the rotor area. The rotating impeller accelerates the incoming fluid and enforces a rotatory motion adding kinetic energy while increasing the pressure due to centrifugal forces (figure 1 and 2). In this case, the impeller consists of five rotating blades dividing the rotor area into five distinct channels C1 to C5 (figure 1). Note, that we will use a fixed clockwise enumeration scheme for the individual channels shown in the right image in figure 1

Evaluation

Contestants had to submit a two-page document describing the visualization and analysis, supplemented by up to 12 images and a video of up to 10 minutes. We received 6 submissions. For each submission, at least 5 reviews were made by 3 domain experts in the field of fluid dynamics and 2 visualization experts. For the best submissions, 2 additional reviews were made by two further domain experts. They evaluated the submissions on clarity, technical soundness, the quality of visualization and interaction, and the value in the field of fluid dynamics.

The Results

The winner was "Visualizing Unsteady Vortical Behavior of a Centrifugal Pump" (Mathias Otto, Alexander Kuhn, Wito Engelke, Holger Theisel). For more on the winner, see the main article.

Honorable mentions went to

"*Visualization of Vortex Core Differences between Ensemble Simulations*" (Alexis Yee Lyn Chan, Joohwi Lee, Russell M. Taylor II).

CEI sponsored an iPad2 for the winner.

Acknowledgments

The data is provided by courtesy of the Institute of Applied Mechanics, Clausthal University, Germany (Dipl. Wirtsch.-Ing. Andreas Lucius). Data hosting is provided by courtesy of SDSC, TeraGrid and the Clausthal University, Germany. The winner prize, an Apple iPad2, was sponsored by CEI. Thanks to Amit Chourasia for his continuous support in the IEEE Visualization Contest.

and a constant x,y perspective for all images of the transport section as the most relevant transport processes occur in the impeller area. During movement, the impeller distributes the incoming fluid among all channels and accelerates the flow in direction of the transport area. There the flow travels at high speed on circular path lines towards the outlet geometry which is illustrated in figure 4. The main goal for engineering such devices is to optimize the flow throughput among varying speed and load settings. In general this implies that recirculation areas have to be avoided [1]. Such areas correlate with vortex structures within the channels and the in- and outflow areas.

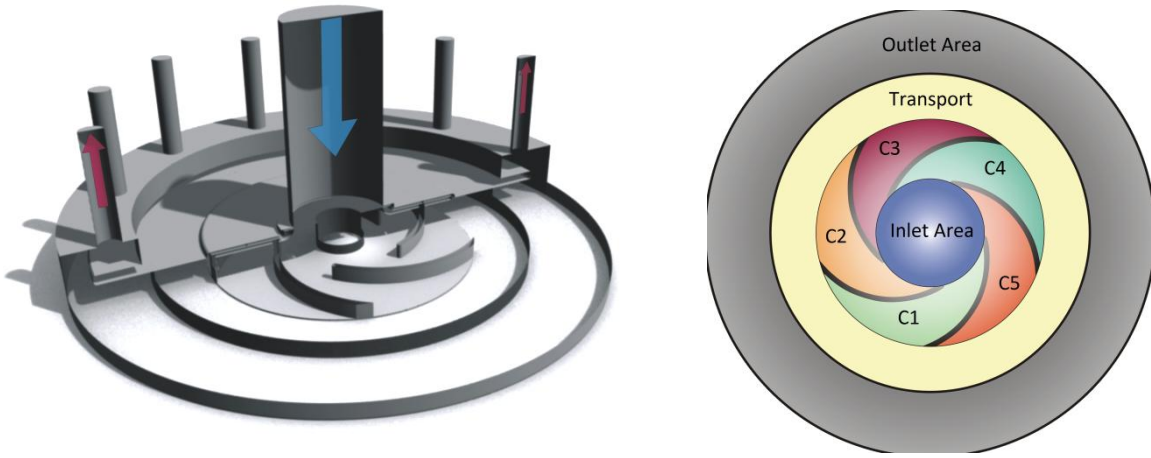


Figure 1: (left) Illustration of the functional principle of the pump. (right) segmentation of functional parts. C1 to C5 denote the separate transport channels.

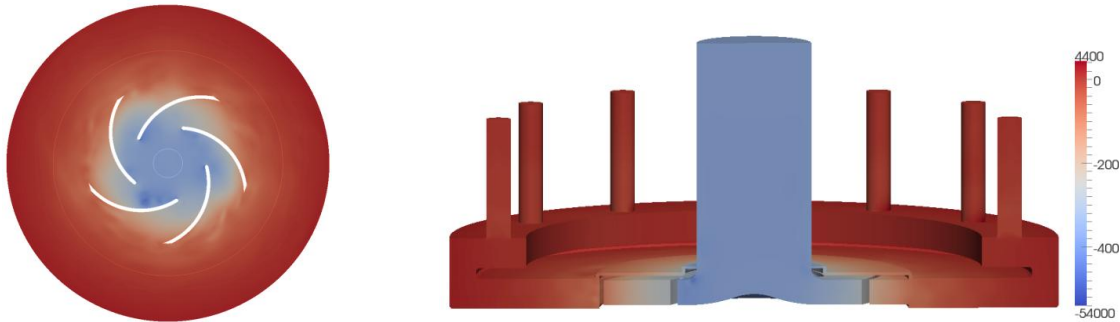


Figure 2: Cross sections of the pressure field. Minima are correlated to vortex cores. A large gradient from the center towards the boundary complicates an automatic analysis.

2.2 Inlet Behavior

The pumping device is characterized by a substantial pressure increase while particles move towards the outlet area shown in figure 2. Minima in the local pressure values are thought to correlate to centers of rotating flow motions. However, we found that these local minima did not in fact correlate with the results of the vortex extractors. These local minima were therefore found to be of little utility in our analysis (e.g. C2). They do not provide information about the overall impact of those features regarding the aforementioned functional aspects. Considering the flow behavior in the inlet area, the distribution into the channels seems nearly equal. However, having a closer look at the inlet boundary reveals flow portions moving backward close to the boundary of the system which is not obvious from the respective scalar fields. This becomes visible looking at the path lines seeded between inlet and transport region as shown in figure 4 and can be explained due to the pressure compensation within the back flow channel above the rotor and the inadequate outflow rate of the pump.

2.3 Transport Behavior

The transport area connects the inlet to the outlet area of the device. In this part two major processes dominate the functionality of the machine: First, a distribution of the incoming flow among all channels. Second, the transport of the flow out of the channels into the outlet area. In an ideal setting both distribution processes should be rotationally-symmetric and have equal volume fractions among all

channels. In the simulation the device operates below optimal rotational speed according to its design. This induces the creation of large turbulent vortex structures and subsequently dominant recirculation areas. This effect is known as *rotating stall* and directly decreases the efficiency of the machine and may lead to an asymmetric load balance among all channels [2].

Figure 2 illustrates that from the local pressure field alone no direct conclusions about the long-term flow behavior can be drawn. Thus, we utilized a set of approaches to extract local vortex core regions. We applied those methods to the SAS simulation model, as it is assumed to have the most realistic turbulence behavior.

Two popular and physically motivated methods to extract vortex regions are the λ_2 criterion [4] and the Q-Criterion [5]. The extraction results are shown in figure 3 in the first two rows. Both approaches utilize a decomposition of the local Jacobian of the velocity into a symmetric component \mathbf{S} and antisymmetric component $\mathbf{\Omega}$. Note that the velocity relative to the impeller motion is considered. The λ_2 criterion is the 2nd largest eigenvalue of the matrix $\mathbf{S}^2 + \mathbf{\Omega}^2$ and the Q criterion is given as $\frac{1}{2}(\|\mathbf{\Omega}\|^2 + \|\mathbf{S}\|^2)$. In both cases level sets of the resulting scalar fields describe regions with vortical behavior. For the λ_2 criterion we are interested in regions with an iso-value smaller than zero (blue regions in figure 3), and for the Q criterion regions larger than a given iso-value (white regions in figure 3).

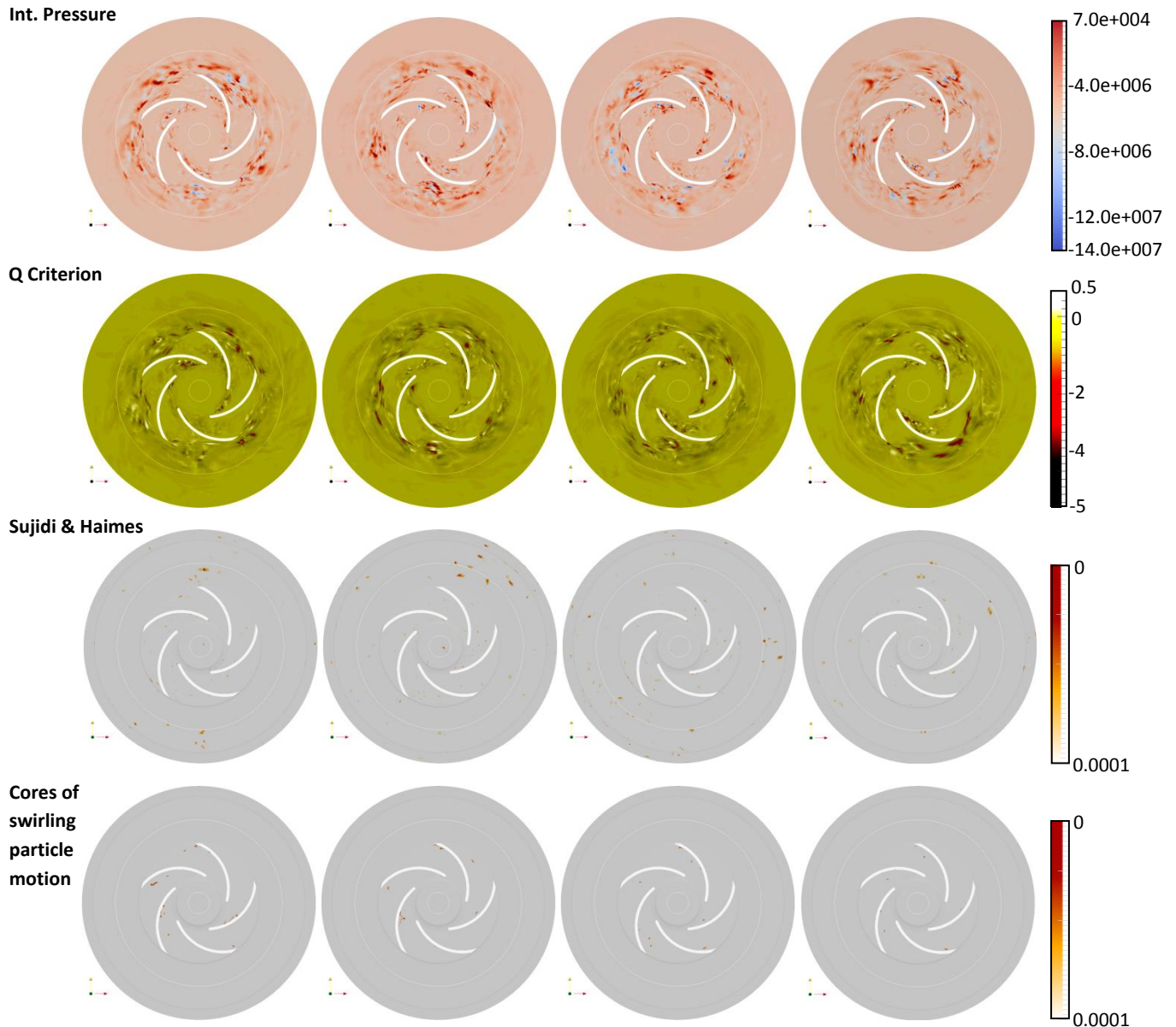


Figure 3: Local vortex criteria for time steps 0, 25, 50, 80. (1st row) λ_2 criterion, (2nd row) Q criterion, (3rd row) method by Sujudi and Haimes, (4th row) cores of swirling particle motion.

In addition to this we applied the more recent vortex criterion proposed by Sujudi and Haimes [6] to gain additional insight into the structure of the vortex regions. This approach is designed to extract vortex core lines. To identify such locations we extract isolated points of zero curvature. The original approach was defined by an analysis of the eigenvectors of the Jacobian. A more common way to find such locations is the use of the Parallel Vectors Operator by Peikert and Roth [8]. Here we have to find locations where the Jacobian of the velocity field \mathbf{v} has two imaginary eigenvalues and the velocity field is parallel to the acceleration field:

$$\mathbf{v} \parallel (\nabla \mathbf{v}) \mathbf{v}$$

An extension to this approach is the so-called 'cores of swirling particle motion' proposed by Weinkauff et al. [7]. This approach additionally considers the unsteady aspect by using the temporal derivatives of the velocity field.

Both results are shown in the last two rows in figure 3. Note, that both criteria are reformulated using a parallel vectors definition that only give a binary information about vortex locations which can be extracted as line structures in an additional post-processing step. We simplified these computations by searching for small angles between the vectors.

The application of those local definitions reveals significant differences in the areas and locations of strong recirculation zones. While the Q and λ_2 criteria extract numerous vortical regions in every time step, more specific locations are identified by Sujudi and Haimes and cores of swirling particle motion. Still, neither a direct statement about blocked channels can be made nor a more global quantification of vortex areas can be provided. In addition to this, Lucius et al. [2] presents an advanced and physically motivated overview about a variety of measures including a global frequency analysis.

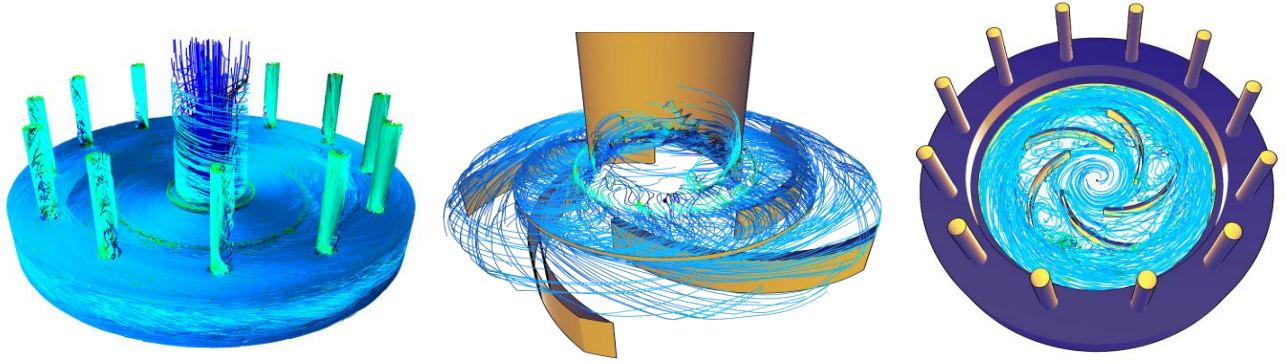


Figure 4: Color-coded path lines: Particles on dark blue path lines move downwards, on cyan colored path lines upwards. Inlet and outlet regions reveal flow portions moving against the expected direction.

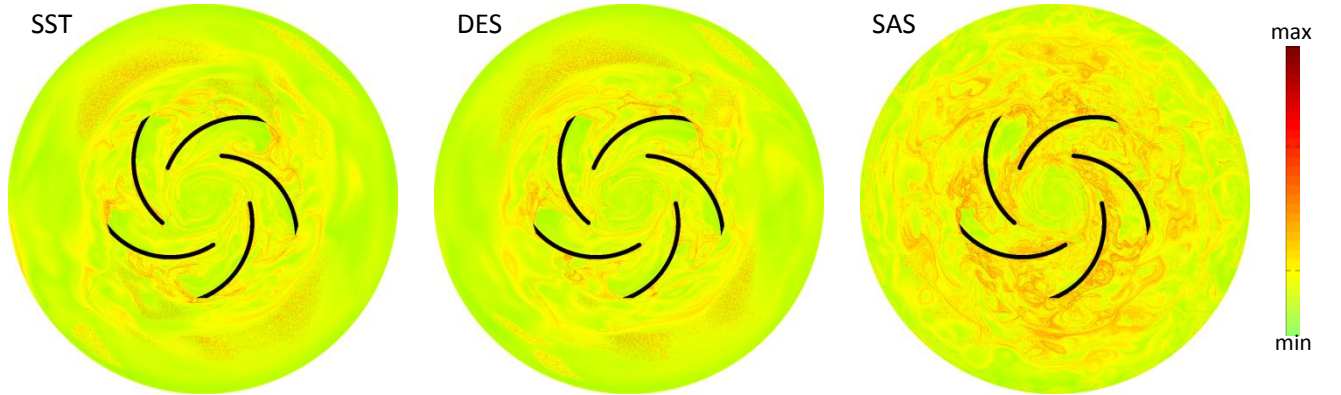


Figure 5: Finite-Time Lyapunov Exponent computed over the whole given time interval (one rotation of the impeller) showing regions of strong separation as ridge structures (red).

As indicated by the application of the local methods the long term behavior of the flow is of special importance in this case. Basic insight into this global and time-dependent behavior is given by the visualization of path lines (figure 4). Color coding the path lines using the z component of the vector field allows to visually separate particles moving up or downward. This color coding emphasizes path lines moving against the direction implicated by the functional principle of the pump. Besides, we can observe vortex structures, but the visualization itself does not allow for a quantification of these effects.

In order to quantify those effects we applied a set of integration based methods that observe the global unsteady flow behavior over a given time interval along path lines. One way of observing the separation behavior is to extract Lagrangian Coherent Structures (LCS). A common definition for visualizing LCS is the Finite-Time Lyapunov Exponent (FTLE) [3]. This approach is based on the flow map $\phi_{t_0}^{t_0+T}$ that defines the transport of particles for each location \mathbf{x} starting at a time t_0 over a time interval T . To obtain information about the local separation rate a variation of the Cauchy-Green deformation is computed by using the gradient of the flow map:

$$\nabla = \left(\frac{d\phi_{t_0}^{t_0+T}(\mathbf{x})}{d\mathbf{x}} \right)^* \cdot \frac{d\phi_{t_0}^{t_0+T}(\mathbf{x})}{d\mathbf{x}}$$

The FTLE value is evaluated by the time-normalized logarithm of the largest eigenvalue of this matrix:

$$\sigma_{t_0}^T(\mathbf{x}) = \frac{1}{|T|} \ln \sqrt{\lambda_{\max}(\nabla)}$$

Locally high values by means of ridges in the resulting scalar field represent areas of highest particle separation, while local minima indicate vortex core regions as shown in figure 5. Note that the resulting scalar field may exceed the resolution of the underlying vector field by far.

In addition to this separation analysis we applied a texture advection method to reveal the transport behavior among the different channels of the data set. Using the given velocities in the respective frame of reference we integrate the regional information encoded in a predefined volume texture to obtain a quantitative statement about the flow distribution among the channels, potential blocking and recirculation effects (see figure 6). Looking into the details of the SAS model we can see that channels C2, C3, and C5 are blocked. The advected texture allows to observe the development of small vortices at the suction side of the impeller blade tips. Due to these vortices the particles move into the subsequent channels C1 and C4, while vortices in the remaining channels grow. In practice this phenomenon correlates to a rotating stall as described previously. In figure 7 we use same technique but with a radial gradient texture. This input texture emphasizes particles moving into

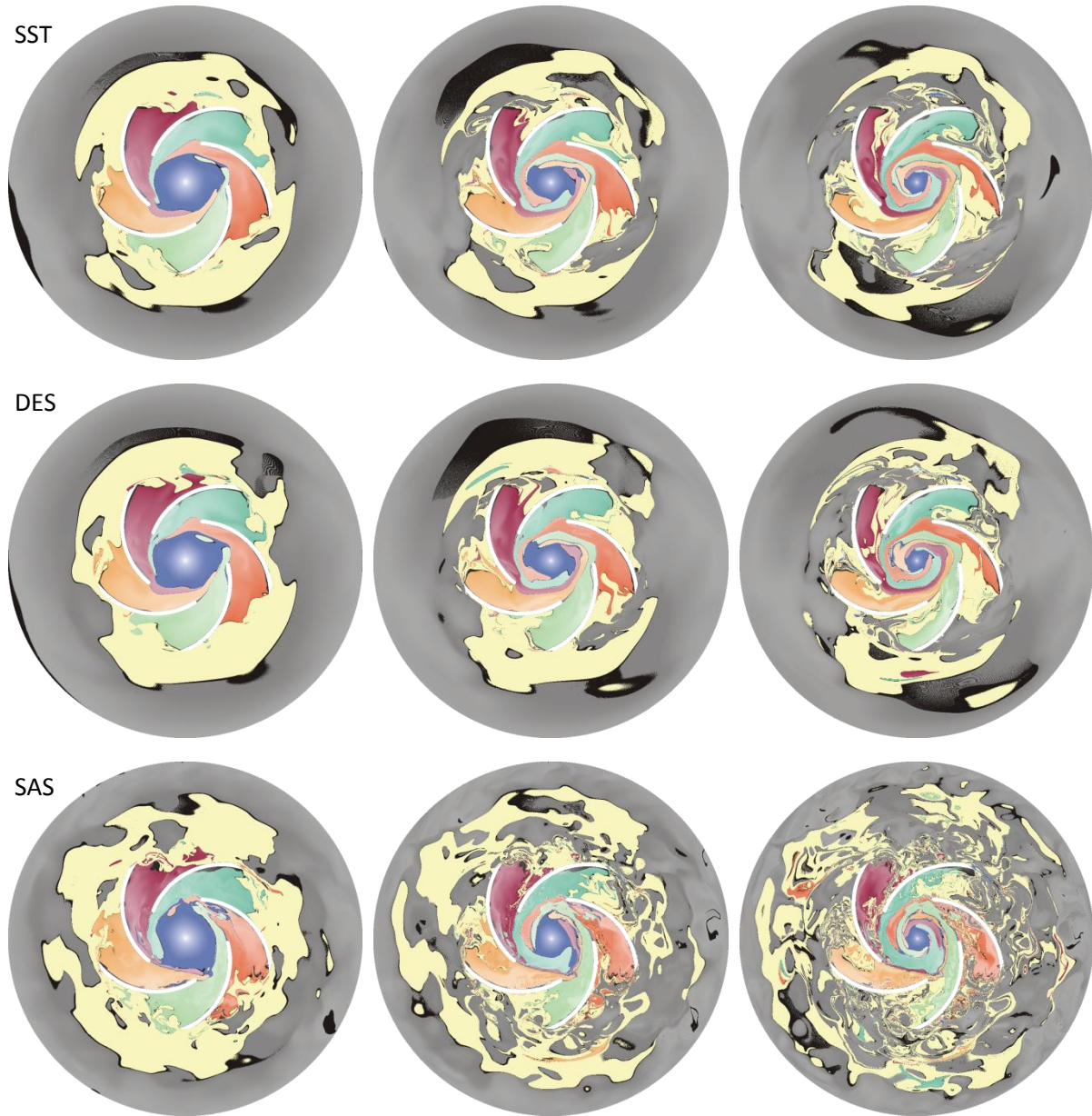


Figure 6: Texture advection using a texture that segments functional parts of the pump (see figure 1 right). The shown time intervals are 20, 50 and 80 starting from time step 0.

inward or outward direction, as areas of flow moving outward become darker, while inward moving portions become brighter during advection.

In addition to the aforementioned methods we observed the integral behavior of the given scalar quantities along time-dependent particle traces. A direct indicator of the long-term differences between flow regions is the arc length of the resulting path lines. It reveals flow separations structures and particles remaining close to the center of vortex regions which is illustrated in figure 8. Further, we accumulated the given pressure along the path lines resulting in a description of its long-term behavior during the circulation (see figure 9). Note that all scalar fields for the Lagrangian methods are computed in the relative velocity frame, while for FTLE the absolute frame would lead to the same results.

3 SIMULATION MODEL COMPARISONS

With the data set three different simulation models were given, namely Scale-Adaptive Simulation (SAS), Detached Eddy Simulation (DES), and Shear Stress Transport (SST). The main difference between those is the modeling of turbulence. In order to illustrate variances we applied our aforementioned integration based methods to all three simulation models as shown in figures 5 to 8. In all cases longer integration times directly reflect the degree and effect of turbulence over the considered time interval in the resulting scalar fields. All Lagrangian methods reveal a significantly more complex turbulence behavior for the SAS model. Additionally, the blocking of individual channels and the components of specific vortex areas cannot be observed in the DES and SST model.

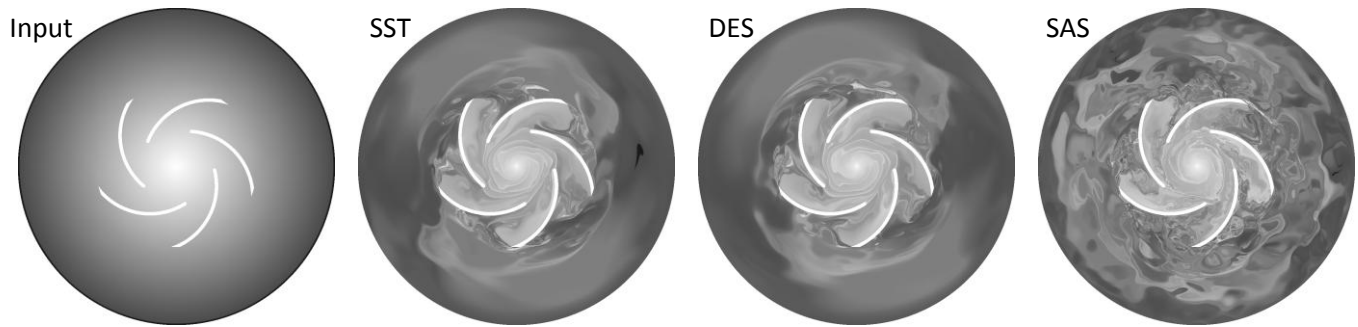


Figure 7: Texture advection with a radial gradient texture for one rotation of the impeller.

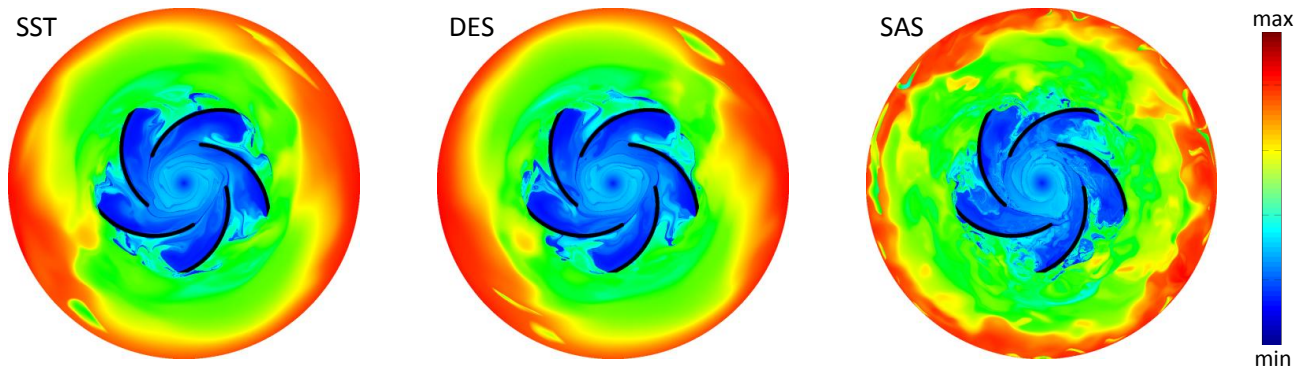


Figure 8: Arc length of path lines during one rotation of the impeller. Blue regions indicate low values and red regions high values.

4 IMPLEMENTATION

To obtain our results we implemented a software prototype to convert, load and process the given data. We used a notebook with an Intel I7 2820QM (8 cores) and 16 GB RAM as test system. The first step to handle the large amount of data was the conversion from ASCII to binary Enight format (only 22.2 GB per model instead of 142 GB). Our C# prototype is accelerated by the Task Parallel Library that allows for multi core processing. The program loads all time steps of the vector data set and one scalar field for each model separately. For the interpolation inside the hexahedral cells we use the Mean-Value Coordinate method equivalent to the one used in the ParaView Toolkit. The integration within the velocity fields is done using a lower order Runge-Kutta scheme. Slices of pre-computed local measures like Q , λ_2 , Sujudi Haines or Swirling Cores are evaluated in real time, while pre-computing those measures for the complete volume takes about one minute. Lagrangian methods seeded at all vertices of the whole volume require about one minute per integration step. However, the resolution of the given grid is too coarse to represent the delicate structures produced by these methods. Thus, we compute integration based methods on slices with a dense uniform distribution of path lines. In addition to our tool we visualize our results using the open-source tool ParaView3.

CONCLUSION

In this work we applied distinct visualization techniques to analyze flow processes inside a centrifugal pump. Our focus was on the identification of cells of rotating stall between the impeller blades. Those vortex structures potentially block complete channels of the impeller and drastically decrease the efficiency of the pump.

Using established local methods we extracted regions with vortical behavior and cores of vortices. Because of the nature of local methods numerous short-term features are extracted, which are in mostly irrelevant for the analysis of rotating stall itself. To overcome those shortcomings, we applied a set of global path line based methods to extract global features over a finite-time interval. Our analysis further revealed portions of the flow moving against the expected flow direction due to the insufficient transport rates caused by recirculation effects. By using FTLE, the arc length of path lines, and the accumulated pressure on path lines we observed a variety of indicators for long-living vortical structures. The most intuitive results we achieved by the texture advection of a volume texture that segmented functional parts of the pump. In this case this technique directly visualizes blocked channels and gives information about the evolution of the rotating stall phenomenon.

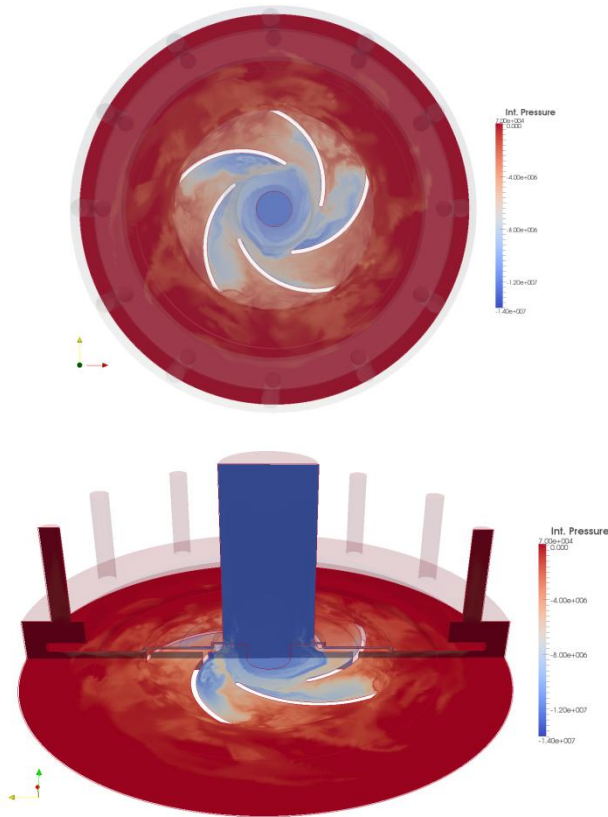


Figure 9: Pressure integrated on path lines during one rotation of the impeller. Minima of this field correspond to particles remaining in low pressure areas for a longer time period. This hints on vortex regions that persist over the respective time interval.

ACKNOWLEDGEMENTS

The project SemSeg acknowledges the financial support of the Future and Emerging Technologies (FET) program within the Seventh Framework Program for Research of the European Commission, under FET-Open grant number 226042.

REFERENCES

[1] G. A. Lucius. Unsteady cfd simulations of a pump in part load conditions using scale-adaptive simulation.

International Journal of Heat and Fluid Flow, 31:1113–1118, 2010.

[2] G. A. Lucius. Numerical simulation and evaluation of velocity fluctuations during rotating stall of a centrifugal pump. Journal of Fluids Engineering, 133:081102, 2011.

[3] G. Haller. Lagrangian coherent structures and the rate of strain in twodimensional turbulence. Phys. Fluids, 30(13):3365–3385, 2001.

[4] J. Jeong. On the identification of a vortex. Journal of Fluid Mechanics, 285:69–94, 1995.

[5] Hunt, J. C. R., Wray, A. & Moin, P. 1988 Eddies, stream, and convergence zones in turbulent flows. Center for Turbulence Research Report CTR-S88.

[6] D. Sujudi and R. Haimes. Identification of swirling flow in 3D vector fields. Technical report, Department of Aeronautics and Astronautics, MIT, 1995.

[7] T. Weinkauff, J. Sahner, H. Theisel, H.-C. Hege, and S. H.-P. Cores of swirling particle motion in unsteady flows. IEEE Transactions on Visualization and Computer Graphics, 13(6):1759–1766, 2007.

[8] R. Peikert, M. Roth, The "Parallel Vectors" Operator — A Vector Field Visualization Primitive, *Proceedings of IEEE Visualization '99*, (San Francisco, CA, USA, October 24-29, 1999), IEEE Computer Society Press, pp. 263-270, 1999.

Mathias Otto is a PhD Student at the University of Magdeburg's Visual Computing Group, otto@isg.cs.ovgu.de

Alexander Kuhn is a PhD Student at the University of Magdeburg's Visual Computing Group, akuhn@isg.cs.ovgu.de

Wito Engelke is a PhD Student at KAUST's Geometric Modeling and Scientific Visualization Center, wito.engelke@kaust.edu.sa

Holger Theisel is the Leader of the University of Magdeburg's Visual Computing Group, theisel@isg.cs.ovgu.de

Thereas-Marie Rhyne at theresamarierhyne@gmail.com